Natural protein engineering in the Ω-loop: the role of Y221 in ceftazidime and ceftolozane resistance in *Pseudomonas*-derived cephalosporinase

Andrew R. Mack, Vijay Kumar, Magdalena A. Taracila, Maria F. Mojica, Margaret O'Shea, William Schinabeck, Galen Silver, Andrea M. Hujer, Krisztina M. Papp-Wallace, Shuang Chen, Shozeb Haider, Emilia Caselli, Fabio Prati, Focco van den Akker, and Robert A. Bonomo

This file contains Figures S1 – S8 and Table S1.

Figure S1. Electrospray ionization mass spectrometry (ESI-MS) of pure PDC-3, PDC-3 E219K, and PDC-3 Y221H incubated with TOL for 30 s at a 1:50 molar ratio. The presence or absence of Methionine (Met; 131 Da) is an artifact of the protein production process. Mass accuracy is ±5 Da. Several observed peaks corresponding to acyl-enzyme complexes were between 14 and 18 Da larger than predicted by loss of the R2 group (as is expected with CAZ and TOL). This additional adduct may represent i) the oxidation of methionine, a common modification seen in mass spectrometry experiments corresponding to the addition of 16 Da (80), ii) the Michael Addition of water across an α,β-unsaturated imine formed following hydrolysis, as has previously been reported for other cephalosporin/β-lactamase combinations (81), or iii) another mechanism not clearly discernible under the current experimental conditions. This observation does not affect our interpretation of the results of the experiments.

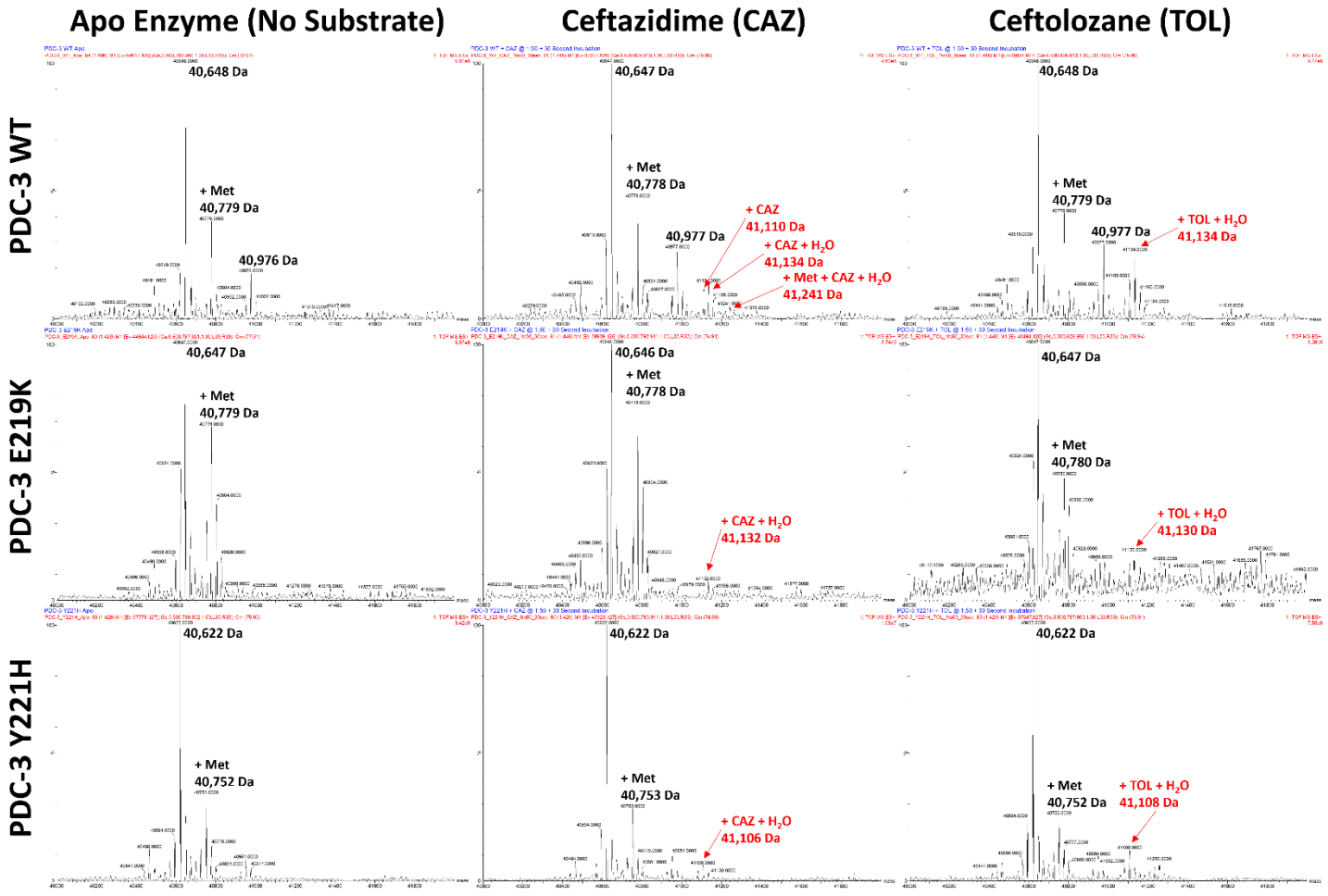

Figure S2. Timed ESI-MS of pure PDC-3, PDC-3 E219K, and PDC-3 Y221H incubated with CAZ for 5 s to 300 s tracking the formation and depletion of the acyl-enzyme complex.

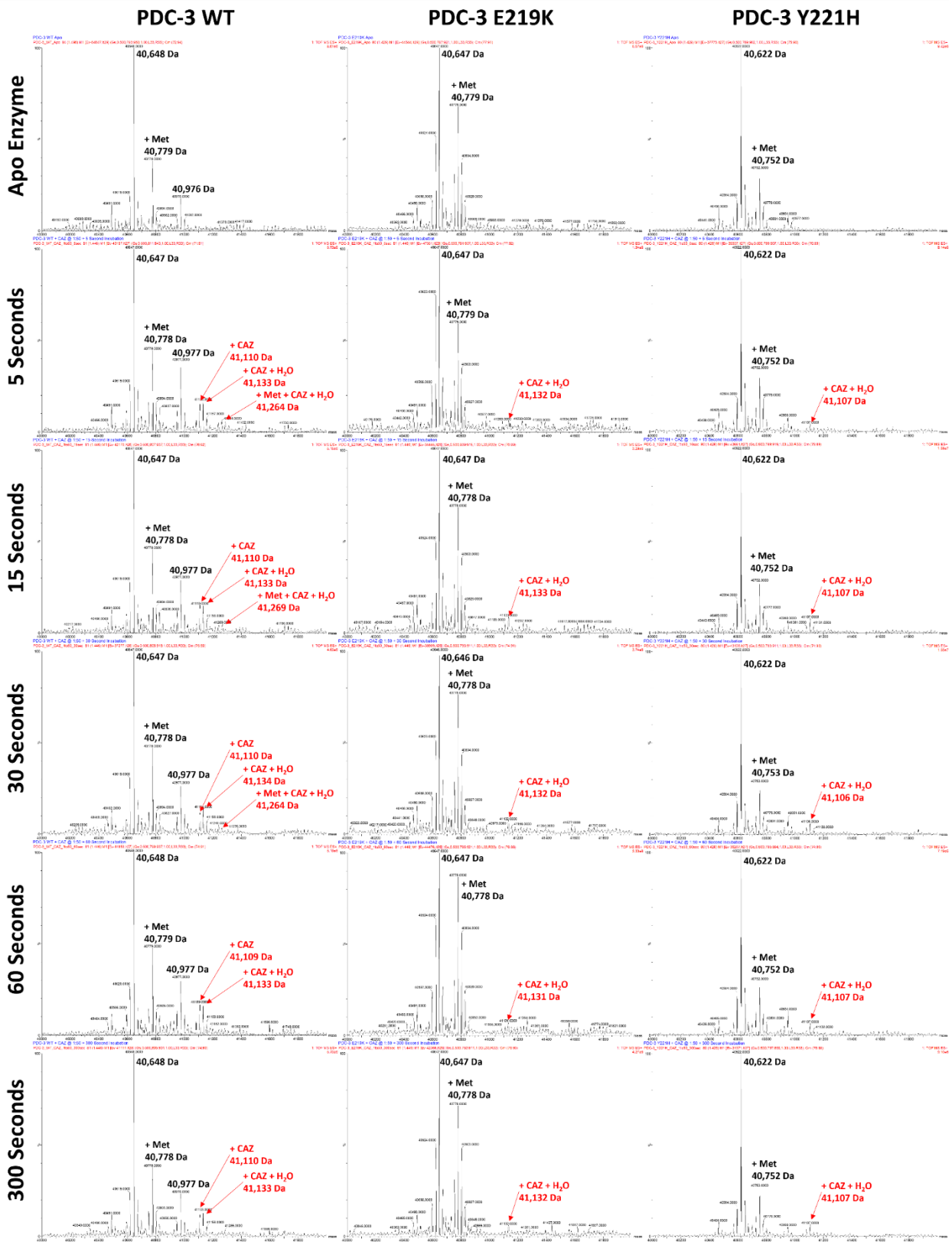

Figure S3. Timed ESI-MS of pure PDC-3, PDC-3 E219K, and PDC-3 Y221H incubated with TOL for 5 s to 300 s tracking the formation and depletion of the acyl-enzyme complex.

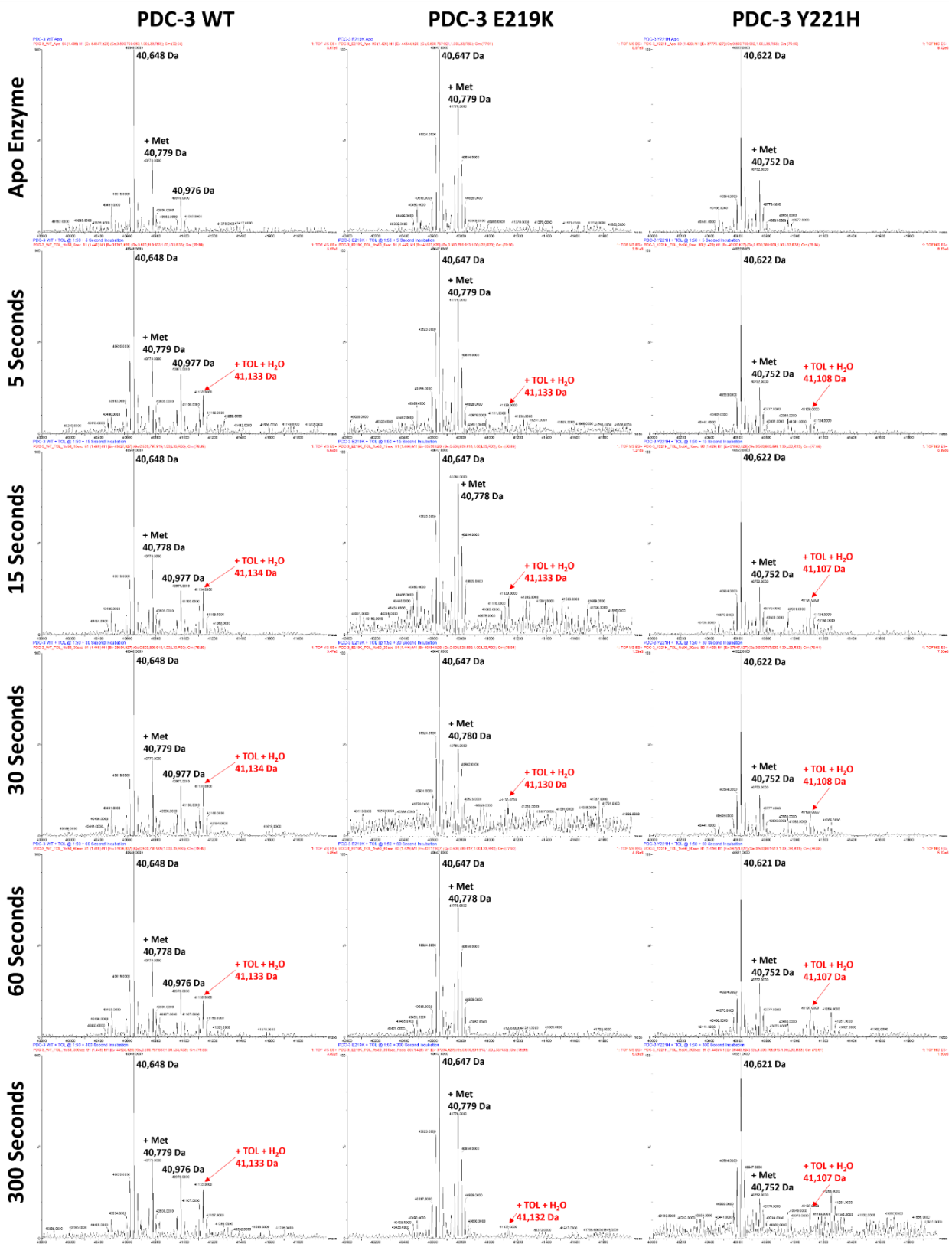

Figure S4. Structure of ligands (A) CAZ (yellow) and (B) TOL (orange) docked into the active site pocket of PDC-3 (green). Ligands are shown in ball-and-stick model and key active site residues are labelled and shown in stick model. Active site hydrogen bonds of CAZ and TOL are indicated by gray dashed lines.

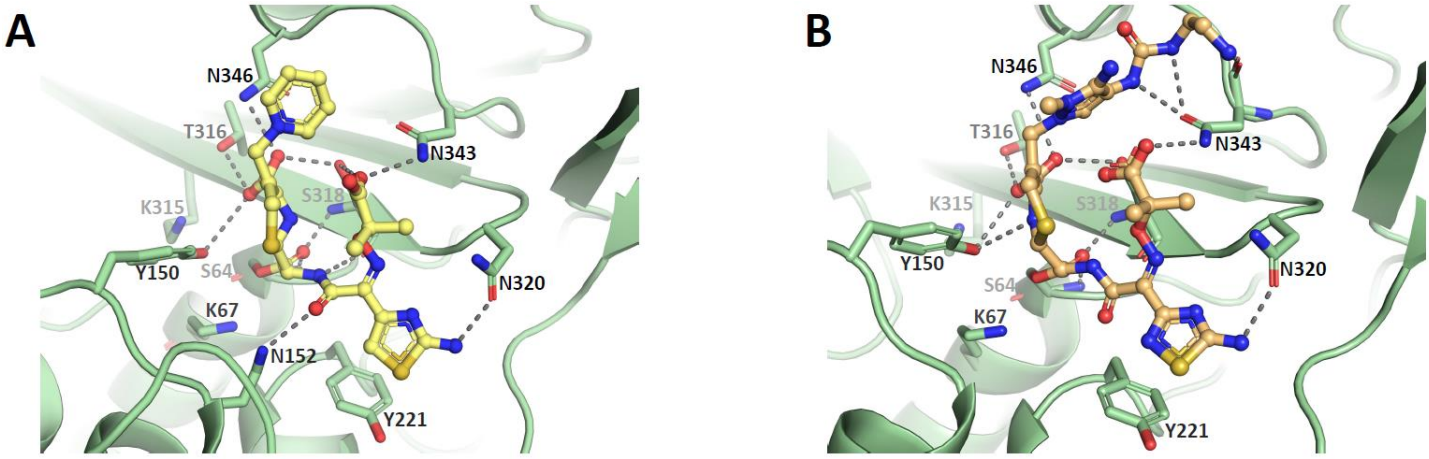

Figure S5. Structure of ligands CAZ and TOL docked into the active site pocket of PDC-3 Y221H (cyan). Panels A-B and their coloring, cartoon representation and labelling same as Figure S4.

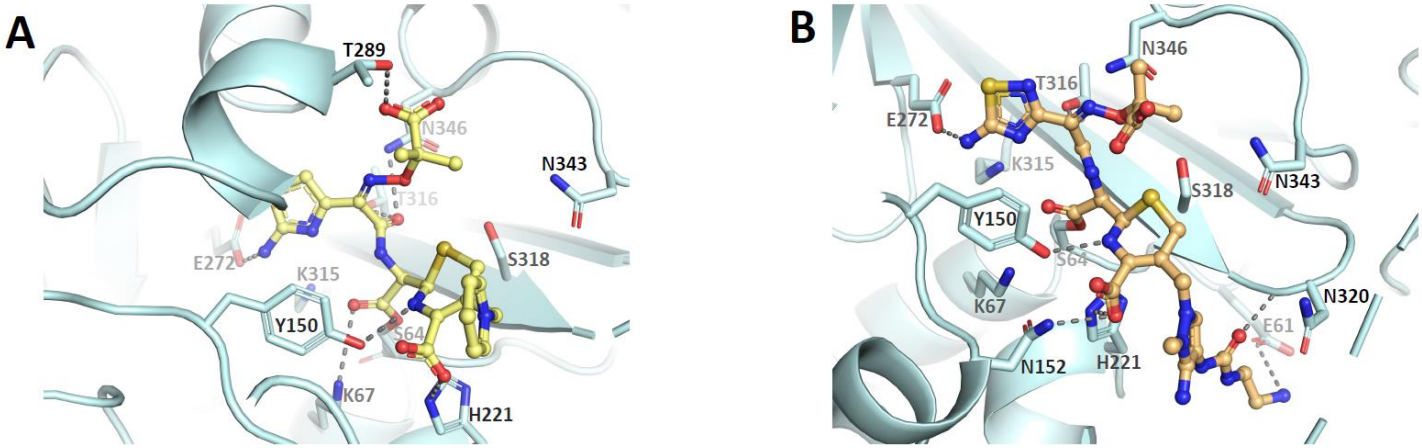

Figure S6. Superposition of (A) CAZ docked into the active site pockets of PDC-3 (green) and PDC-3 Y221H (cyan), and (B) TOL docked into their active site pockets, coloring scheme like panel A. Ligands are shown in ball-and-stick model, colored identical to their respective protein partner, and residues Y221/ H221 are labelled and shown in stick model with black curved-arrow indicating flipping of side chain towards the catalytic residue S64 in PDC-3 Y221H mutant.

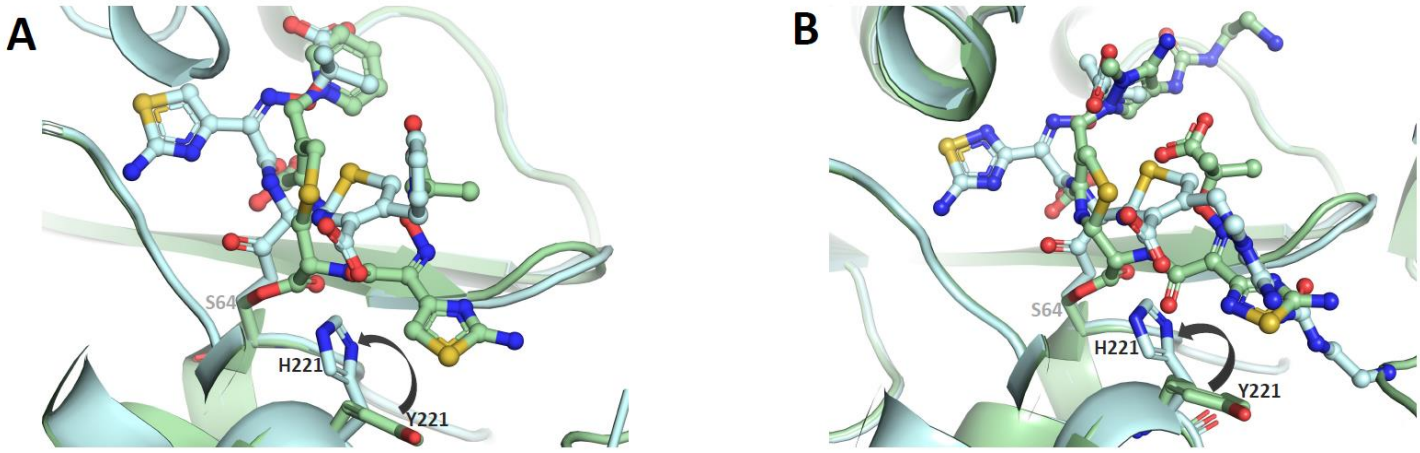

Figure S7. Convergence of WTMetaD for PDC-3. Diffusibility of (A) CV1 (Φ) and (C) CV2 (ψ) over simulation time. Projection of the free-energy (FE) on collective variables (B) CV1 (Φ) and (D) CV2 (ψ). (E) Gaussian height (kcal/mol) vs simulation time plotted.

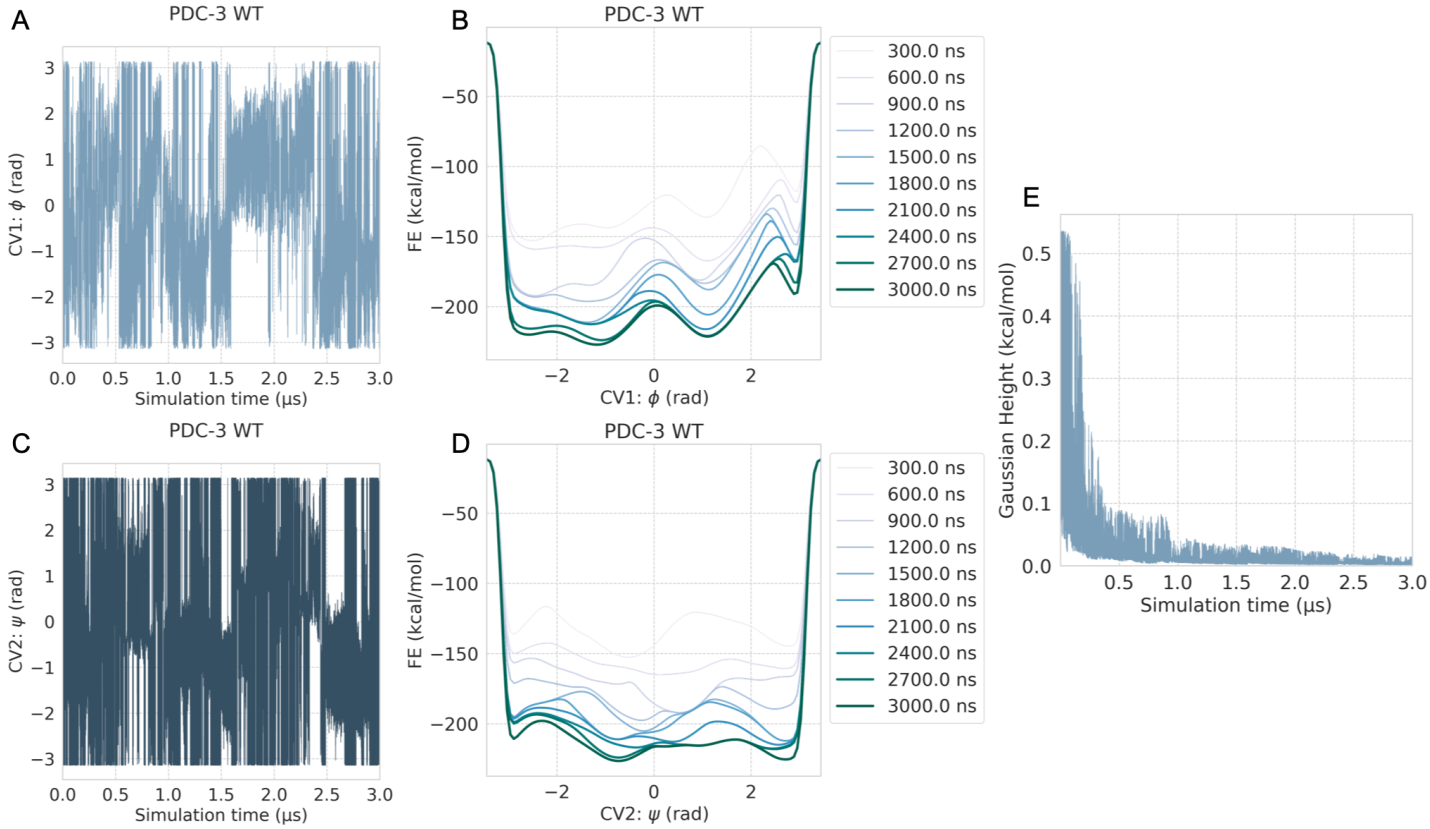

Figure S8. Convergence of WTMetaD for the Y221H variant. Diffusibility of (A) CV1 (Φ) and (C) CV2 (ψ) over simulation time. Projection of the free-energy (FE) on collective variables (B) CV1 (Φ) and (D) CV2 (ψ). (E) Gaussian height (kcal/mol) vs simulation time plotted.

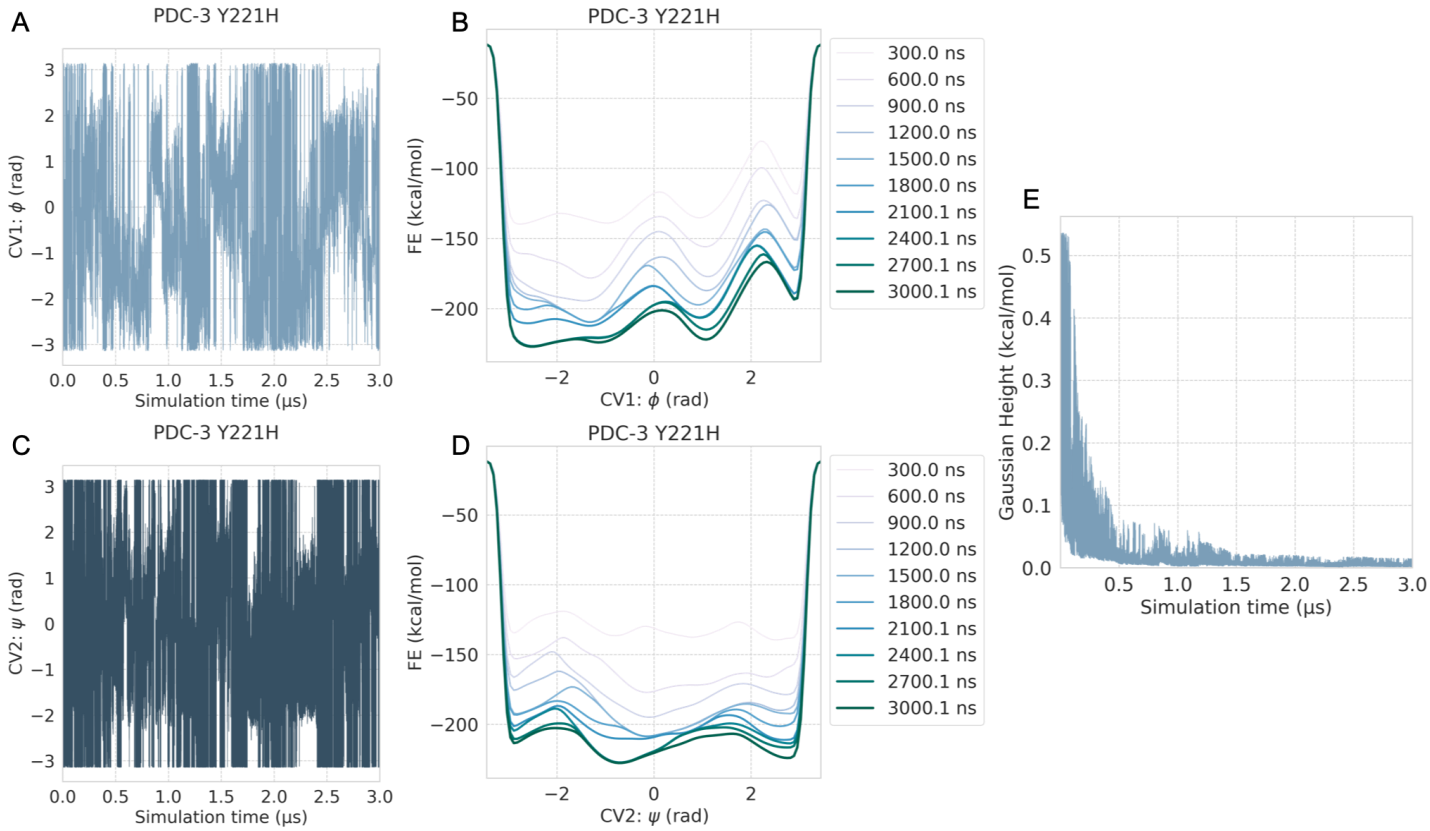

Table S1. Docking scores of CAZ and TOL with PDC-3 and PDC-3 Y221H β-lactamases using the Schrodinger software suite.

Protein	CAZ	TOL
PDC-3	-6.137	-7.834
PDC-3 Y221H	-5.653	-6.306